Open Archive Toulouse Archive Ouverte (OATAO)

OATAO is an open access repository that collects the work of Toulouse researchers and makes it freely available over the web where possible.

To link to this article :
URL : http://dx.doi.org/10.1016/j.susc.2007.01.015

Any correspondence concerning this service should be sent to the repository administrator: staff-oatao@inp-toulouse.fr

Density functional theoretical study of Cu_n, Al_n ($n = 4$–31) and copper doped aluminum clusters: Electronic properties and reactivity with atomic oxygen

Corinne Lacaze-Dufaure [*], Christine Blanc, Georges Mankowski, Claude Mijoule

CIRIMAT, ENSIACET, UMR CNRS 5085, 118 route de Narbonne, 31077 Toulouse Cedex 4, France

Abstract

A DFT study of the electronic properties of copper doped aluminum clusters and their reactivity with atomic oxygen is reported. Firstly we performed calculations for the pure Cu_n and Al_n ($n = 4, 9, 10, 13, 25$ and 31) clusters and we determined their atomization energy for some frozen conformations at the B3PW91 level. The calculated work functions and M–M (M = Cu, Al) bond energies of the largest clusters are comparable with experimental data. Secondly, we focused our attention on the change of the electronic properties of the systems upon the substitution of an Al atom by a Cu one. This latter stabilizes the system as the atomization energy of the 31-atoms cluster increases of 0.31 eV when the substitution is done on the surface and of 1.18 eV when it is done inside the cluster. We show that the electronic transfer from the Al cluster to the Cu atom located at the surface is large (equal to 0.7 e^-) while it is negligible when Cu is inserted in the Al_n cluster. Moreover, the DOS of the Al_{31} and $Al_{30}Cu$ systems are compared. Finally, the chemisorption energies of atomic oxygen in threefold sites of the Al_{31}, Cu_{31} and $Al_{30}Cu$ clusters are calculated and discussed. We show that the chemisorption energy of O is decreasing on the bimetallic systems compared to the pure aluminum cluster.

1. Introduction

Copper-containing aluminum alloys such as 2024 alloy are often used in aerospace applications; thus, there is significant interest in their corrosion behaviour in aerated solutions. These materials are high-strength alloys in which a heterogeneous microstructure is developed by thermomechanical processing to obtain good mechanical properties. In such alloys, copper is present in the matrix as well as in various fine strengthening phases and coarse intermetallic particles. For instance, 2024 alloy is characterized by a mean copper content of the matrix of about 4 wt.% (a quasi pure aluminum matrix containing about 0.02 wt.% Cu and strengthening copper-rich particles) and coarse intermetallic particles with high Cu concentrations [1,2]. Due to the high influence of copper on the oxidation and electrochemical behaviour of copper-containing aluminum alloys [3,4], it is interesting to study in details models of the pure Al and Cu phases as well as the binary AlCu phases.

Models for the theoretical treatment of crystalline solids and surfaces were reviewed by Batra and Kleinman [5] and more recently by Jug and Bredow [6]. The authors classified the models as finite systems and periodic approaches. We are interested by the former ones. In the cluster model, it is assumed that a surface can be represented adequately by a finite number of atoms; the main difficulty arising from this approach is the border effects. Two ways were developed, i.e. saturation and embedding, in order to avoid this problem. Another solution is to use cluster large enough to get reasonable models of the surface. This

[*] Corresponding author. Tel.: +33 5 62 88 57 05; fax: +33 5 62 88 56 00.
E-mail address: Corinne.Dufaure@ensiacet.fr (C. Lacaze-Dufaure).

method allows obtaining a concrete description of the electronic density localization as well as the eventual charges transfers by using atomic orbitals. On the other hand, the periodic approach often by using a plane waves basis set allows to have a better description of the band structure of the infinite systems.

Our goal is to study the electronic properties of copper containing aluminum alloys and their reactivity with oxygen. More precisely, the possible dissociative chemisorption of molecular oxygen is studied. Indeed, it was previously shown that a molecular physisorbed state exists on the Al(111) surface [7,8]. But it was also demonstrated experimentally [5,9,10] and theoretically [5,7,8,11] that molecular oxygen dissociates on Al surfaces almost spontaneously. The chemisorption of the O atoms is thus commonly considered as the initial step of the oxidation process of the Al surface [7,11–13].

Copper and aluminum containing systems were the purpose of many theoretical studies in the literature. Without being complete, we focus our literature review here on that dealing with Cu and Al pure- and bimetallic systems in the framework of the density functional theory (DFT).

Pure copper clusters were investigated in order to determine size effects on their geometrical structure and electronic properties [14–26]. The size of the studied clusters varies between 2 and 13 Cu atoms with one work dealing with larger cluster up to 32 atoms [27]. Copper clusters were also widely used to model the Cu surface and its reactivity against atomic or molecular species [28–37]. Periodic studies dealing with the surface and the bulk of the metallic systems were also described [21,38–41]. Furthermore, the same approach was used to investigate the adsorption of atomic and molecular oxygen [30,42–47].

Aluminum clusters were also the purpose of many works where the authors focused on the geometrical and electronic properties of Al_n clusters [48–60]. Periodic calculations on aluminum systems, i.e. aluminum atomic chains, bulk metal and the infinite surface, are also available [61–65]. The initial stage of oxidation of the (111) surface of aluminum was also studied. Early experimental and theoretical studies were discussed by Batra and Kleinman [5]. This exhaustive review was followed by several works on the adsorption and dissociation of the oxygen molecule and the stability of aluminum oxide films [7,8,11–13,66].

Doped copper clusters were also the purpose of much work with studies on NiCu [67], PdCu [68–70], RhCu [71], PtCu [72], CoCu [73–75] and AuCu [76] systems. The cluster model was specially chosen by Illas et al. to studied the bonding mechanism between atoms in PdCu alloys using the Pd_1Cu_{12}, Pd_4Cu_6, Pd_8Cu_{92} and $Pd_{40}Cu_{60}$ clusters [69,70]. Dealing with periodic systems, Ruban et al. presented a database of the surface segregation energies in transition metal alloys including copper alloys, derived from LDA-DFT computations in conjunction with a tight-binding representation [77]. Slab DFT calculations are also available for the PdCu, PtCu and FeCu systems with various compositions [78–84].

There are few studies on doped aluminum systems [85–94]. For example, calculations were carried out on Fe_nAl_m ($n + m = 15$) clusters [85] or on $(FeAl)_n$ ($n \leqslant 6$) clusters [86].

Copper doped aluminum clusters were studied by Khanna et al. [95] and Zope and Baruah [96] who looked for their equilibrium geometries. We also found several studies whose aim is to model the Al and AlCu surfaces using both cluster-like approach and slab computations. For instance, the adsorption of copper atoms on two Al_{25} and Al_{37} frozen clusters modelling the Al(100) surface was investigated and an adsorption energy of 3.52 eV was calculated. The authors also conclude that there is no clear indication of a charge transfer mechanism for the bonding as they did not see any charge transfer between the substrate and the adsorbate [97].

Others authors claimed that the adsorption of a copper atom can restore the reactivity of the oxidized Al surface, modelled by a two-layer Al_{18} cluster [98]. Periodic LDA computations were performed by Wolverton et al. who calculated the energetic properties of the Al_2Cu θ and θ′ phases and incorporated them in computational thermodynamics approaches [99,100].

The present work is aimed at studying the properties and the reactivity of Cu doped Al clusters in relation to the reactivity of AlCu alloys. In order to simulate the metal and the infinite surface, we first present studies on frozen Cu_n, Al_n and $Al_{30}Cu$ clusters. These preliminary computations are benchmarks in order to determine the dependence of some properties of the bimetallic systems due to the Al substitution by Cu. In a second part, we investigate the reactivity of the pure and bimetallic AlCu systems with atomic oxygen. Firstly, the adsorption is done on frozen Al_{31}, Cu_{31} and $Al_{30}Cu$ clusters. It is related to our goal to simulate the O adsorption on a (111) surface of an fcc structure. Secondly, we take into account the local cluster relaxation when O is adsorbed on its surface. To our knowledge, no previous study has been reported on that subject. The relative adsorption energies of O and charge distributions on the systems are compared and discussed.

2. Computational details

The calculations were performed in the framework of the density functional theory using the GAUSSIAN98 package [101]. In this study, the exchange part of the functional is treated with the Becke's three parameters functional (B3) [102]. The correlation part is described by the Perdew and Wang (PW91) GGA functional [103]. The so-called B3PW91 has proved to be suitable to describe such kind of systems [19,20]. Los Alamos National Laboratory effective core potentials as well as a DZ atomic basis sets are used for Al and Cu, treating explicitly 3 and 19 electrons, respectively [104–106]. The O atom is treated with the D95 full DZ basis set.

Broken-symmetry calculations were performed in order to take into account the spin polarization and the results

presented here concern the systems in their more stable spin state (three spin states were explored for each system).

The clusters are built along the (1 1 1) plane and kept frozen (Cu–Cu bond length = 2.555 Å and Al–Al bond length = 2.857 Å [107]). For the pure Cu_n systems, we use two-layers (Cu_4, Cu_9, Cu_{10}, Cu_{25}) and three-layers (Cu_{10}, Cu_{13}, Cu_{31}) clusters. The Al_n systems are also described by two-layers (Al_4, Al_9, Al_{10}, Al_{25}) and three-layers (Al_{13} and Al_{31}) clusters. The clusters with $n = 4$–25 are presented in Fig. 1 while the clusters with $n = 31$ are shown in Fig. 2. The Al_{31} cluster is taken as the reference to study the $Al_{30}Cu$ systems in which a copper atom substitutes an aluminum one in two different position successively (Fig. 2). In position no. 1, the copper atom is situated in the surface layer whereas it is surrounded by 12 neighbours when placed in position no. 2.

The atomization energy per atom of a pure M_n cluster (M = Cu and Al) containing n atoms is defined by

$$E_{atomization} = \frac{nE(M) - E(M_n)}{n}$$

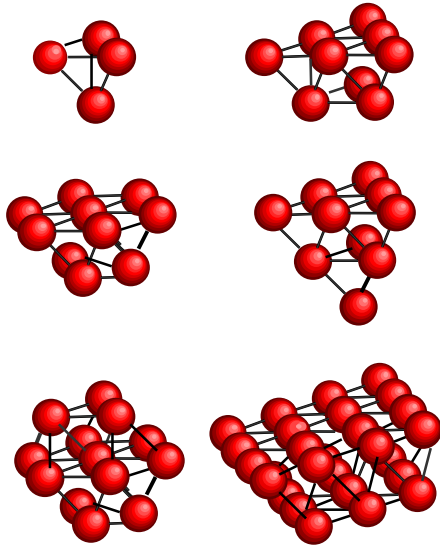while the M–M binding energy is given by

Fig. 1. Clusters geometries used for the calculations on the Al_n and Cu_n ($n = 4, 9, 10, 13$ and 25) pure systems.
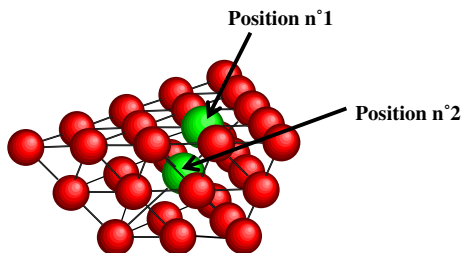

Fig. 2. Geometry of the MAl_{30} (M = Al, Cu) cluster used for the substitution of a Al atom by a Cu atom, in two successive positions (position nos. 1 or 2).
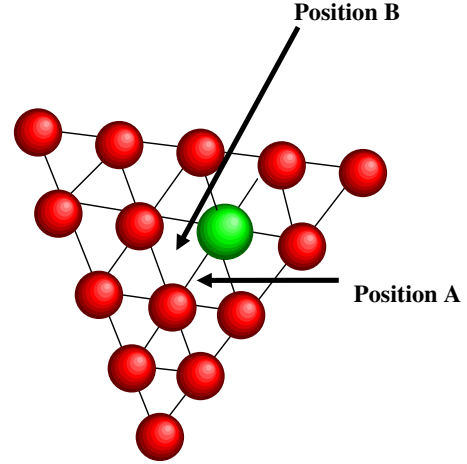

Fig. 3. The O adsorption sites on the first layer of the MAl_{30} (M = Al, Cu) cluster.

$$E_{bond} = \frac{nE(M) - E(M_n)}{N}$$

where N is the number of M–M bonds in the cluster.

We can also extrapolate from the M–M binding energy in the cluster an estimation of the bulk cohesive energy, as

$$E_{cohesion} = 12^*(E_{binding}/2)$$

For the bimetallic $Al_{30}Cu$ systems, the atomization energy is defined as

$$E_{atomization} = 30E(Al) + E(Cu) - E(Al_{30}Cu)$$

and the copper extraction energy is

$$E_{extraction} = E(Al_{30}) + E(Cu) - E(Al_{30}Cu)$$

For all the systems, the work function ϕ is determined from the Fermi energy as described in Ref. [108]. From the discrete distribution of the energy levels for the clusters, we plot the density of state (DOS) using the GaussSum package [109].

The O atom is adsorbed on the surface in pure or mixed threefold sites on the Cu_{31}, Al_{31} and $Al_{30}Cu$ clusters (see Fig. 3). The O atom is placed either above the threefold (A) or threefold (B) sites. The former one has no atom on the z-axis in the second layer while the latter does. We first perform computations with the metal cluster kept frozen. The vertical O–metal distance above the surface varies to optimize the O–Al and O–Cu bonds. Secondly, we take into account the local relaxation of the cluster with O adsorption: the O atom and its metallic nearest neighbours are allowed to relax.

In both case, we determined the O binding energy:

$$E_{binding} = E(cluster) + E(O) - E(O\text{-}cluster)$$

3. Results and discussion

We begin this article with a discussion on the change of the electronic properties of the pure Cu_n and Al_n clusters

with cluster size. It is followed by the study of the bimetallic systems and their reactivity against oxygen.

3.1. Pure Cu_n and Al_n clusters

The structure of the Cu_n and Al_n ($n = 4$–31) clusters are shown in Figs. 1 and 2. The results concerning the Cu_n clusters in their most stable spin state are given in Table 1. The total energy is given together with the calculated atomization energy per atom, the Cu–Cu binding energy and the work function determinated from the Fermi energy. The most stable spin states of Cu_n are doublet states when n is odd (except for the Cu_{31} cluster) and triplet states when n is even. The atomization energy per atom ranges from 1.03 to 2.15 eV increasing with the size n of the cluster. The convergence to the bulk value (3.50 eV [107]) is slow and comparable to that of the number of bonds per atom (see Table 1). The optimized cluster structures from the literature are very different in shape than the frozen cluster used in this work. Nevertheless the atomization energy per atom of copper calculated for the optimized or nonoptimized clusters are not so different [15,18–27]. We also plot for comparison the atomization energy per atom and the cohesive energy estimated for the bulk from the averaged Cu–Cu binding energy (Fig. 4). The latter decreases rapidly to the experimental value of 3.50 eV for the bulk metal. The value of 3.84 eV calculated from the Cu–Cu binding energy of the largest Cu_{31} cluster compares well with the cohesive energy determined from periodic computations, i.e. 3.89 eV (PW91 [39]) or 3.74 eV (FLAPW/PBE [41]).
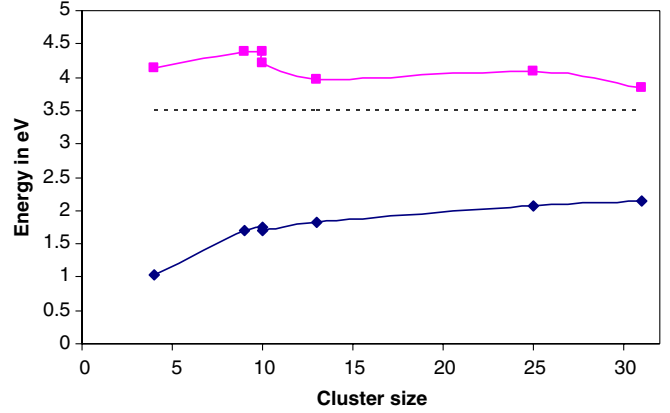

Fig. 4. Comparison of the atomization energy per atom of the clusters (–◇–) and their cohesive energy (–□–) calculated from the Cu–Cu binding energy (B3PW91 level). Dash line: experimental value for the bulk metal [107].

While the ionization potential of the clusters (calculated as 5.54 eV for the largest Cu_{31} cluster) strongly overestimates the experimental value of the work function for an infinite surface, the calculated work function of 4.54 eV for the largest cluster compares well with the experimental value of 4.65 eV [107]. The reasonable simulation of the properties of the infinite surface by a frozen Cu(111) cluster is also related to the experimental and theoretical evidences that the Cu(111) surface does not reconstruct [39,40] or weakly reconstruct [41, and Ref. therein].

Finally, we looked at the electronic configuration of the copper atoms inside the cluster, by means of a Mulliken

Table 1
Energetic properties (absolute energy in ua, atomization energy per atom and Cu–Cu binding energy in eV) and calculated work function ϕ of the Cu_n clusters at the B3PW91 level

Systems	Number of bond per atom	Multiplicity	Abs. energy (ua)	$E_{atom.}$ per atom (eV)	E binding Cu–Cu (eV)	ϕ (eV)
Cu		2	−196.154262			
Cu_4 – 2 layers	1.5	3	−784.768575	1.03	0.69	5.50
Cu_9 – 2 layers	2.3	2	−1765.951221	1.70	0.73	4.18
Cu_{10} – 2 layers	2.4	3	−1962.183482	1.74	0.73	4.70
Cu_{10} – 3 layers	2.4	3	−1962.162294	1.69	0.70	4.74
Cu_{13} – 3 layers	2.8	2	−2550.877008	1.82	0.66	4.36
Cu_{25} – 2 layers	3.0	2	−4905.745070	2.07	0.68	4.40
Cu_{31} – 3 layers	3.4	4	−6083.227561	2.15	0.64	4.54
Cu_8 – 2 layers[a,b]	1.6	1	−1569.7215	1.66	0.95	4.49
Cu_9 – Cs sym[a,c]	2.4			2.06		
Cu_9 – Cs sym[a,d]	2.4			1.77		
Cu_{10}[a,e]	2.0			2.00		
Cu_{13} – C1 sym[a,f]		2		1.74		
Cu_{13}[a,g]	2.3			2.00		
Experiment [107]	12			3.50	0.58	4.65

[a] Optimized geometry.
[b] From Ref. [19] (LANL2DZ/B3PW91).
[c] From Ref. [15] (PW91).
[d] From Ref. [20] (LANL2DZ/B3PW91).
[e] From Ref. [27] (LANL2DZ/PBE).
[f] From Ref. [23] (LANL2DZ/B3LYP).
[g] From Ref. [21] (PW91).

Table 2
Energetic properties (absolute energy in ua, atomization energy per atom and Al–Al binding energy in eV) and calculated work function ϕ of the Al_n clusters at the B3PW91 level

Systems	Number of bond per atom	Multiplicity	Abs. energy (ua)	$E_{atom.}$ per atom (eV)	E binding Al–Al (eV)	ϕ (eV)
Al		2	−1.940501			
Al_4 – 2 layers	1.5	5	−7.927824	1.13	0.75	6.19
Al_9 – 2 layers	2.3	2	−17.997848	1.61	0.69	4.74
Al_{10} – 2 layers	2.4	3	−20.050941	1.76	0.73	5.07
Al_{13} – 3 layers	2.8	2	−26.159414	1.95	0.70	5.00
Al_{25} – 2 layers	3.0	4	−50.379406	2.03	0.67	4.86
Al_{31} – 3 layers	3.4	2	−62.558428	2.11	0.62	4.78
Al_{10}[a]	2.3	3		1.90		
Al_{11}[a]	2.8	2		1.99		
Experiment [107]	12			3.34	0.56	4.24

[a] Optimized geometry; from Ref. [53] (LANL2DZ/BPW91).

population analysis. The configuration of the isolated copper atom is $(3d^{10}4s^14p^0)$. We observe an electronic transfer from the 4s atomic orbital to the 4p orbital with the increasing size of the cluster (Cu_4: $3d^{9.85}$ $4s^{0.85}$ $4p^{0.30}$, Cu_{10}: $3d^{9.80}$ $4s^{0.65}$ $4p^{0.49}$ and Cu_{13}: $3d^{9.80}$ $4s^{0.28}$ $4p^{0.91}$), while the 3d orbital occupation remains nearly constant.

The results concerning the Al_n ($n = 4$–31) pure clusters are presented in Table 2. The first difficulty with aluminum arises with the description of the lowest electronic state of the isolated atom for which the electronic configuration is $(3s^23p^1)$. It corresponds to two different electronic states $^{1/2}P_{1/2}$ and $^{1/2}P_{3/2}$ and thus each of them is described by a multireferential wave function. Nevertheless, the energy gap between the $^{1/2}P_{1/2}$ and $^{1/2}P_{3/2}$ electronic states is only 0.014 eV [110] and we can expect that the monodeterminantal character of the DFT wave function (which is a mixing between both "true" electronic states) leads to an available electronic energy. In Table 2 and in Fig. 5, we can see for the same reasons as in the case of the Cu_n clusters that the atomization energy per atom increases slowly to the experimental counterpart of 3.34 eV [107]. The equilibrium geometries of optimized clusters are different in shape than our frozen systems. But the confrontation be-

tween the values of the atomization energy per atom of our frozen systems and that calculated with optimized clusters [53] shows comparable results. The cohesive energy estimated from the Al–Al binding energy of the largest Al_{31} cluster (0.62 eV) is of 3.72 eV. It is in better agreement with experiments and the value of the cohesive energy of 3.50 eV determined from GGA periodic computations [7,8]. The work function converges slowly to the experimental work function of 4.24 eV for an infinite aluminum surface [107]. It is a better estimation that the crude determination of the ionization potential (5.65 eV for the Al_{31} three-layer cluster).

From these results, the largest cluster Cu_{31} and Al_{31} are assumed to describe reasonably the electronic properties of the metal. Their reactivity upon adsorption will be investigated in the next sections.

3.2. Clean bimetallic $Al_{30}Cu$ systems

We used the $Al_{30}Cu$ clusters to simulate the true alloy [4] in order to reduce border effects that could influence the adsorption process on smaller clusters. The shape of the cluster was chosen to present A and B threefold adsorption sites (see Fig. 3). As the position of the copper in the Al matrix may be a key factor to the surface reactivity, we substituted successively one Al atom by a Cu atom in two different positions (nos. 1 and 2 on Fig. 2), leading to two different $Al_{30}Cu$ clusters. The Cu atom is located in the surface layer for one cluster (Cu position no. 1), and it is inside the cluster with 12 Al–Cu bonds in the second one (Cu position no. 2). The results of our calculations are given in Table 3. They show that the total atomization energy of the $Al_{30}Cu$ systems is higher than that of the Al_{31} cluster ($\Delta E_{atomization} = 0.31$ eV and 1.18 eV). The $Al_{30}Cu$ clusters are more stable than the Al_{31} cluster. Furthermore, the cluster where the Cu atom is surrounded by 12 Al neighbours is the most stable system: the extraction energy is of 2.99 eV and of 3.79 eV for Cu in position 1 and 2, respectively. This behaviour is in agreement with previous results that were about optimized small Al_nCu ($n = 11$–14) clusters [95,96].
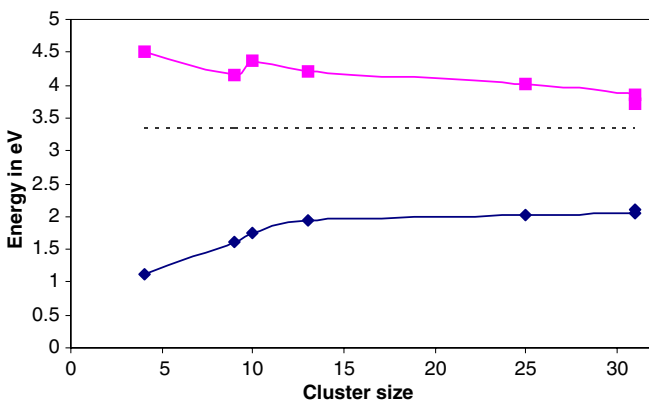

Fig. 5. Comparison of the atomization energy per atom of the clusters (–◇–) and their cohesive energy (–□–) calculated from the Al–Al binding energy (B3PW91 level). Dash line: experimental value for the bulk metal [107].

Table 3
Energetic properties, calculated work function ϕ and relative Mulliken net charges of the Al_{31}, Cu_{31} and $Al_{30}Cu$ clusters at the B3PW91 level

Systems	Pos. of Cu atom	Mult.	Absolute energy (ua)	ΔE_{atom}[a] (eV)	Cu extraction energy[b] (eV)	$\Delta E_{extr.\ per\ bond}$[c] (eV)	ϕ (eV)	$\Delta q_{X/Al}$[d] (in e)	ΔQ_{layer}[e] (in e)
Al_{31}		2	−62.558428				4.78		
Cu_{31}		4	−6083.227561				4.54		
$Al_{30}Cu$	1	2	−256.784042	0.309	2.994	0.036	4.67	$\Delta q_{Cu(1)/Al(1)} = -0.73$	1st layer: −0.45
									2nd layer: +0.47
									3rd layer: −0.02
$Al_{30}Cu$	2	4	−256.815881	1.176	3.791	0.099	4.74	$\Delta q_{Cu(2)/Al(2)} = -0.02$	1st layer: −0.21
									2nd layer: +0.25
									3rd layer: −0.04

[a] $\Delta E_{atomization} = E_{atomization}\,(Al_{30}Cu) - E_{atomization}\,(Al_{31})$.
[b] $E_{extraction} = E(Al_{30}) + E(Cu) - E(Al_{30}Cu)$; the Al_{30} clusters are taken in their most stable state (triplet).
[c] Gain of energy for a Cu–Al bond when compared to a Al–Al bond in Al_{31}
$\Delta E_{extraction\ per\ bond} = (Cu\ extraction\ energy\ in\ Al_{30}Cu - Al\ extraction\ energy\ in\ Al_{31})/N$. N: number of Cu–Al bonds in the $Al_{30}Cu$ cluster.
[d] $\Delta q_{X/Al} = q_X\ (X = Cu\ and\ Al\ in\ Al_{30}Cu) - q_{Al}\ (corresponding\ position\ in\ Al_{31})$
q: atomic Mulliken net charges. The numbering Cu(i) and Al(i) (i = 1, 2) corresponds to the position nos. 1 and 2 in the clusters (see Fig. 2).
[e] $\Delta Q_{layer} = Q_{layer}\ (in\ Al_{30}Cu) - Q_{layer}\ (in\ Al_{31})$; Q: global Mulliken net charges for the layer.

We also want to estimate the gain of energy of an M–Al bond, replacing one atom M = Al by M = Cu in the Al_{31} clusters in position 1 and 2. We calculated:

$$\Delta E_{extraction\ per\ bond} = (Cu\ extraction\ energy\ in\ Al_{30}Cu)$$
$$- (Al\ extraction\ energy\ in\ Al_{31})/N$$

with Cu and Al in the same position in the $Al_{30}Cu$ and the Al_{31} systems and N the number of Cu–Al bonds. It shows that a Cu–Al bond is stronger than a Al–Al bond. It is in agreement with the stabilization of the system upon alloying.

The weak variation of the calculated work function with the Cu substitution indicates that the availability of electrons which participate in first to charge transfer in reactivity process remains nearly unchanged. By a Mulliken population analysis, we determined that the electronic transfer arises from the Al host to the Cu atom in the two bimetallic clusters. This is simply explained by comparing the IP of Cu (7.72 eV at B3PW91/LANL2DZ level of theory) with the energy of the LUMO (4.03 to 4.25 eV) of the Al_{30} clusters having the same structure as the $Al_{30}Cu$ systems but with the Cu atom lacking.

We define the relative net charge $\Delta q_{X/Al}$ of an atom X (X = Cu and Al) with an atomic net charge q_X as: $\Delta q_{X/Al} = q_X\ (X = Cu\ and\ Al\ in\ Al_{30}Cu) - q_{Al}\ (same\ position\ in\ Al_{31})$.

For the $Al_{30}Cu$ system, the relative net charge of Cu in position no. 1 is of −0.73 e. This result shows a charge transfer mechanism for the bonding that was not seen in others studies [97,98]. From the relative global net charge of the different layers in the clusters ΔQ_{layer}, we see that the electronic transfer comes from the adjacent layer in the cluster to the Cu atom. The Al–Al bonds are thus weaker in the bimetallic systems than in the Al_{31} pure cluster. When the Cu atom substitutes the Al atom in position no. 2, resulting to a cluster where the Cu atom is surrounded by 12 Al atoms, we note a redistribution of the

electrons within the cluster but the net charge of the central atom (no. 2) remains unchanged.

We plot the electronic density of states (DOS) for the Al_{31} and $Al_{30}Cu$ systems. The full width at half maximum (FWHM) of each peak is here of 0.7. For the Cu atom (doublet/B3PW91), the p-, d- and s-states lie at −75.14, −6.65 and −5.18 eV, respectively. In the Fig. 6 are shown the alpha and beta DOS for the Al_{31} pure cluster and for the more stable $Al_{30}Cu$ system. In this figure, the three levels lying at around −77 eV for each system are not drawn. They correspond to pure Cu p-orbitals. The DOS profiles show that the doping slightly modifies the MO energy levels in comparison to the Al_{31} cluster. The DOS curve for the $Al_{30}Cu$ system is similar to the Al_{31} cluster with extra peaks at around 9 eV. The Mulliken population analysis describes these levels as a combination of Al-s and Cu-s,d orbitals.

3.3. Atomic oxygen adsorption on the Al_{31}, Cu_{31} and $Al_{30}Cu$ clusters

We chose to use cluster models as it was demonstrated in the past that adsorption and reactions on pure metal and alloys surfaces can be reasonably modelled using a cluster-like approach, especially at very low coverage [69–71]. The modification of the reactivity with O when compared to that of the Al pure cluster is described in terms of the adsorption properties (chemisorption energy, distances O–Cu and O–Al) and electronic transfers. The O atom is adsorbed on the surface of the Al_{31}, Cu_{31} and $Al_{30}Cu$ systems (Fig. 3). For the Al_{31} cluster, we investigated A and B adsorption sites. For the $Al_{30}Cu$ cluster with Cu in the surface (position no. 1), the O atom was adsorbed in a mixed (Al/Cu) A site and in a mixed (Al/Cu) B site. For the $Al_{30}Cu$ (Cu position no. 2) system, we chose the B adsorption site. It is composed of solely Al atoms in the first layer with the Cu atom in the second layer. Firstly,
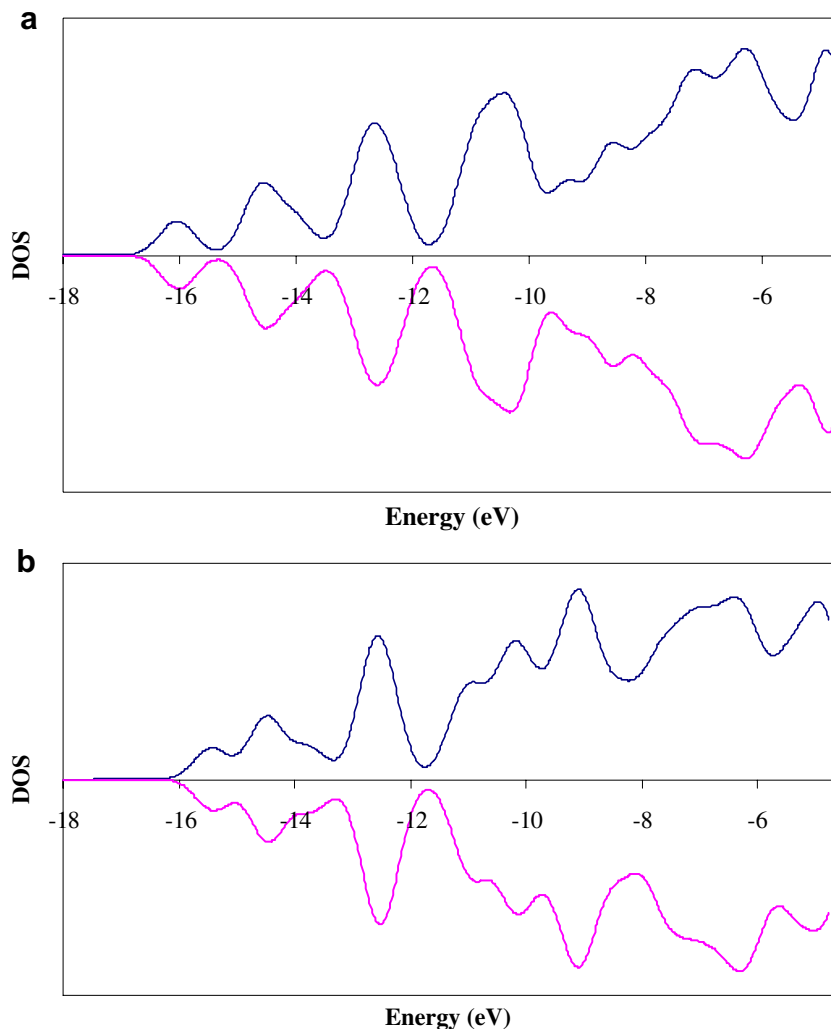
Fig. 6. Alpha (–) and beta (–) DOS for (a) the Al_{31} and (b) the $Al_{30}Cu$ cluster with Cu in position 2 (see Fig. 2) at the B3PW91 level. Only the occupied levels are shown.

the metallic clusters are kept frozen. The results are presented in Tables 4 and 5. They illustrate the influence of the presence and the location of the copper atom on the O adsorption properties. For the Al_{31} cluster, the A adsorption site is favoured with a O binding energy of 5.99 eV to be compared to 5.58 eV for the B site, showing that the chemisorption of molecular oxygen is dissociative (the calculated binding energy of O_2 in the gas phase is equal to 4.09 eV, and the physisorption energy is of the order of 0.2 eV). These values are low if we compare to the DFT periodic results found by several authors that predicted an O binding energy on Al(1 1 1) in the range of 7–10 eV [7,8,11,12,66]. However, the O–Al distance of 1.860 ± 0.005 Å compares well with the O–Al distances determined in these studies and that are in the range of 1.85–1.90 Å [7,8,11,12,66]. These previous periodic computations where performed without constraints. The authors noted that the relaxation of the Al surface layer upon O adsorption can be neglected and lower weakly the O binding energy (−10 to 14 meV) [7,11]. As expected, our

DFT results are higher than the O binding energy found using HF approaches to describe O/Al_n interactions ($E_B = 3.5$ eV [111]).

For the A site, we got an O adsorption energy of 5.64 eV on $Al_{30}Cu$ and of 5.99 eV on Al_{31}. For the B adsorption site, we calculated an O adsorption energy of 5.32 and 5.28 eV on the $Al_{30}Cu$ with Cu in position 1 and 2, respectively, to be compared to 5.58 eV for O on Al_{31}. Thus, the presence of the copper atom in the adsorption site lowers the O chemisorption energy independently of the position of the Cu atom (position nos. 1 or 2). On $Al_{30}Cu$, the A adsorption site is also favoured over the B one. The change in the adsorption energies are in agreement with the change of the distance O–X (X = Al of the adsorption site) of 1.894 and 1.865 Å, respectively, to be compared to 1.855 Å on Al_{31}.

From the Mulliken population analysis, we see a large electronic transfer from the Al_{31} cluster to the O atom ($q_O = -1.00$ e). This transfer is lowered when the adsorbate is directly coordinated to the copper atom ($q_O = -0.83$ e

Table 4
Energetic properties, geometric parameters and relative Mulliken net charges of the OAl$_{31}$, OCu$_{31}$ and OAl$_{30}$Cu clusters (B3PW91 level of theory) – frozen adsorption site

Systems	Ads. site	Mult.	Absolute energy (ua)	O atomic net charge and Δq_X[b]
O		3	−75.052138	
O + Al$_{31}$	B	2	−137.815969	O: −1.00; $\Delta q_{Al\ (site)}$ = +0.41; +0.41; +0.41
	A	2	−137.830936	O: −1.00; $\Delta q_{Al\ (site)}$ = +0.50; +0.50; +0.15
O + Cu$_{31}$	B	4	−6158.412859	O: −0.45; $\Delta q_{Cu\ (site)}$ = −0.01; −0.01; −0.01
	A	4	−6158.406383	O: −0.47; $\Delta q_{Cu\ (site)}$ = −0.23; −0.23; −0.13
O + Al$_{30}$Cu Cu pos. 1[a]	B	4	−332.031756	O: −0.83; $\Delta q_{Al\ (site)}$ = +0.37; +0.37; $\Delta q_{Cu\ (site)}$ = +0.16
	A	4	−332.043337	O: −0.84; $\Delta q_{Al\ (site)}$ = +0.43; +0.20; $\Delta q_{Cu\ (site)}$ = +0.24
O + Al$_{30}$Cu Cu pos. 2[a]	B	4	−332.062031	O: −1.01; $\Delta q_{Al\ (site)}$ = +0.44; +0.44; +0.44; Δq_{Cu} = −0.31

[a] pos.: position of the Cu atom in the cluster, see Fig. 2.
[b] $\Delta q_X = q_X$ (in O-cluster) − q_X (corresponding atom in the clean cluster). X = Cu, Al; q: atomic Mulliken net charges.

Table 5
Energetic properties, geometric parameters and relative Mulliken net charges of the OAl$_{31}$, OCu$_{31}$ and OAl$_{30}$Cu clusters (B3PW91 level of theory) – frozen or *relaxed* adsorption site

Systems	Ads. site	Mult.	Distance O–X[b] (Å)	O adsorption energy (eV)	$\Delta z/z_i$[c] (%)
O + Al$_{31}$	B	2	1.855	5.58	
			1.855	*6.38*	*+25*
	A	2	1.865	5.99	
			1.846; 1.846	*6.68*	*+16*
			O–Al *(border): 1.897*		*+19*
O + Cu$_{31}$	B	4	1.980	3.62	
			1.952	*3.78*	*+8.9*
	A	4	1.962	3.45	
			1.933; 1.933	*3.61*	*+10.3*
			O–Cu *(border): 1.980*		*−0.8*
O + Al$_{30}$Cu Cu pos. 1[a]	B	4	1.894	5.32	
			O–Cu: *2.068*	*5.99*	*−5.6*
			O–Al: *1.815; 1.815*		*+28.3*
	A	4	1.884	5.64	
			O–Cu: *2.049*	*6.16*	*−6.8*
			O–Al: *1.809*		*+15.8*
			O–Al *(border): 1.836*		*+18.4*
O + Al$_{30}$Cu Cu pos. 2[a]	B	4	1.865	5.28	
			1.856	*5.83*	*+25.8*

[a] pos.: position of the Cu atom in the cluster, see Fig. 2.
[b] X: atom of the adsorption site; X = Al and Cu.
[c] $\Delta z/z_i$: vertical relaxation of the atom (relative to the bulk interlayer distance).

on Al$_{30}$Cu (A and B with Cu in position 1)). The copper outermost electrons are less available for the transfer than those of the aluminum atoms. However, the charge variation upon oxidation within the cluster show that the electronic transfer comes in first from the surface layer in interaction with the O atom, and more precisely from the atoms composing the adsorption site. For Cu in position 2, an electronic rearrangement in the cluster occurs upon adsorption as the O and the Cu atoms get both some electrons from the Al host.

On the Cu$_{31}$ cluster (B site), the calculated O binding energy is of 3.62 eV and the electronic transfer of 0.45 e$^-$ towards the adsorbate showing that the O adsorption is less favourable in the presence of copper. It is difficult to compare these results on Cu$_{31}$ with the O chemisorption energy on Cu(1 1 1) available in the literature as the authors do not agree and present results in the range of 1.7–5.0 eV [30,42,43].

We also estimate the local relaxation in the case of O adsorption on the metallic clusters. The results are presented in Table 5 (*italic values*). The O adsorption energies increase significantly when the clusters are allowed to relax locally. The relaxation leads to a shortening of the O–Al and O–Cu distances. The Al$_{31}$ and Al$_{30}$Cu clusters are more influenced by the local relaxation process than the Cu$_{31}$ cluster: the increase of the O adsorption energy (E_{ads} relaxed cluster − E_{ads} frozen cluster) is in eV of +0.80 (site B), +0.69 (site A) on Al$_{31}$, +0.67 (site B – Cu position 1),

+0.52 (site A – Cu position 1), +0.55 (site B – Cu position 2) on $Al_{30}Cu$ to be compared to +0.16 (site A or B) on Cu_{31}. In all case, the A adsorption site is still more stable than the B site. The Al atoms and the Cu atom behave differently as we estimate the vertical displacement $\Delta z/z_i$ of +16 to +25% for Al and from −6.8% to 8.9% for Cu, where z_i is the (1 1 1) interlayer distance. On the other hand, the electronic transfers remain nearly unchanged.

4. Conclusion

We performed density functional computations on Cu_n, Al_n (n up to 31 atoms) and two bimetallic $Al_{30}Cu$ clusters. The calculated work functions and M–M (M = Cu, Al) bond energies of the largest clusters are comparable with experimental data.

For the bimetallic systems, we can conclude that the substitution of an Al atom by a Cu one stabilizes the system as the atomization energy of the 31-atoms cluster increases of 0.31 eV when the substitution is done on the surface and of 1.18 eV when it is done inside the cluster. Comparing Al_{31} and $Al_{30}Cu$, we note that the electron transfer proceeds from the Al cluster to the Cu atom. Moreover, the DOS of the Al_{31} $Al_{30}Cu$ systems are compared. Finally the reactivity of the Al_{31}, Cu_{31}, and $Al_{30}Cu$ clusters with atomic oxygen is investigated. We studied successively frozen and locally relaxed clusters. We note that in all case the A adsorption site is favoured over the B site, in agreement with previous theoretical works. The O adsorption energies increase significantly when the cluster is allowed to relax (+0.16 to +0.80 eV). Independently of the relaxation effects, the substitution of an Al atom by a Cu atom leads to a weakening of the O-cluster binding energy.

Acknowledgements

References

[1] C. Blanc, B. Lavelle, G. Mankowski, Corros. Sci. 39 (1997) 495.
[2] C. Blanc, S. Gastaud, G. Mankowski, J. Electrochem. Soc. 150 (2003) B396.
[3] S. Garcia-Vergara, F. Colin, P. Skeldon, G.E. Thompson, P. Bailey, T.C.Q. Noakes, H. Habazaki, K. Shimizu, J. Electrochem. Soc. 151 (2004) B16.
[4] J. Idrac, C. Blanc, G. Mankowski, M.C. Lafont, G. Thompson, T. Hashimoto, P. Skeldon, Y. Liu, in: P. Schmuki, D.J. Lockwood, Y.H. Ogata, M. Seo, H.S. Sacs (Eds.), Proceedings of the 206th ECS Meeting, Pits and Pores: Formation, Properties and Signifi-
cance for Advanced Materials, PV 2004-19, The Electrochemical Society, Pennington, New Jersey, 2006, p. 218.
[5] I.P. Batra, L. Kleinman, J. Electron Spectrosc. Relat. Phenom. 33 (1984) 175.
[6] K. Jug, T. Bredow, J. Comput. Chem. 25 (2004) 1551.
[7] Y. Yourdshahyan, B. Razaznejad, B.I. Lundqvist, Phys. Rev. B 65 (2002) 75416.
[8] Y.F. Zhukovskii, P.W.M. Jacbs, M. Causa, J. Phys. Chem. Solids 64 (2003) 1317.
[9] J. Trost, H. Brune, J. Wintterlin, R.J. Behm, G. Ertl, J. Chem. Phys. 108 (1998) 1740.
[10] H. Brune, J. Wintterlin, R.J. Behm, G. Ertl, Phys. Rev. Lett. 68 (1992) 624.
[11] J. Jacobsen, B. Hammer, K.W. Jacobsen, J.K. Norskov, Phys. Rev. B 52 (1995) 14954.
[12] A. Kiejna, B.I. Lundqvist, Phys. Rev. B 63 (2001) 85405.
[13] A. Kiejna, B.I. Lundqvist, Surf. Sci. 504 (2002) 1.
[14] P. Calaminici, A.M. Köster, N. Russo, D.R. Salahub, J. Chem. Phys. 105 (1996) 9546.
[15] K. Jug, B. Zimmermann, P. Calaminici, A.M. Köster, J. Chem. Phys. 116 (2002) 4497.
[16] K. Jug, B. Zimmermann, A.M. Köster, Int. J. Quantum Chem. 90 (2002) 594.
[17] C. Massobrio, A. Pasquarello, R. Car, Chem. Phys. Lett. 238 (1995) 215.
[18] C. Massobrio, A. Pasquarello, A. Dal Corso, J. Chem. Phys. 109 (1998) 6626.
[19] P.B. Balbuena, P.A. Derosa, J.M. Seminario, J. Phys. Chem. B 103 (1999) 2830.
[20] P. Jaque, A. Toro-Labbé, J. Chem. Phys. 117 (2002) 3208.
[21] G.H. Guvelioglu, P. Ma, X. He, Phys. Rev. Lett. 94 (2005) 26103.
[22] P. Calaminici, A.M. Köster, A. Vela, J. Chem. Phys. 113 (2000) 2199.
[23] Z. Cao, Y. Wang, J. Zhu, W. Wu, Q. Zhang, J. Phys. Chem. B 106 (2002) 9649.
[24] Y. Shen, J.J. BelBruno, J. Phys. Chem. A 109 (2005) 512.
[25] H. Hakkinen, M. Moseler, U. Landman, Phys. Rev. Lett. 89 (2002) 33401.
[26] H. Gronbeck, P. Broqvist, Phys. Rev. B 71 (2005) 73408.
[27] M. Yang, K.A. Jackson, J. Chem. Phys. 122 (2005) 184317.
[28] M.A. van Daelen, M. Neurock, R.A. van Santen, Surf. Sci. 417 (1998) 247.
[29] J. Torras, C. Lacaze-Dufaure, N. Russo, J.M. Ricart, J. Mol. Catal. A 167 (2001) 109.
[30] Y. Okamoto, Chem. Phys. Lett. 405 (2005) 79.
[31] B. Gomes, J.A.N.F. Gomes, F. Illas, J. Mol. Catal. A 170 (2001) 187.
[32] J.M. Phillips, F.M. Leibsle, A.J. Holder, T. Keith, Surf. Sci. 545 (2003) 1.
[33] G.C. Wang, L. Jiang, Y. Morikawa, J. Nakamura, Z.S. Cai, Y.M. Pan, X.Z. Zhao, Surf. Sci. 570 (2004) 205.
[34] H. Ostrom, A. Fohlisch, M. Nyberg, M. Weinelt, C. Heske, L.G.M. Pettersson, A. Nilsson, Surf. Sci. 559 (2004) 85.
[35] K. Itoh, T. Kiyohara, H. Shinohara, C. Ohe, Y. Kawamura, H. Nakai, J. Phys. Chem. B 106 (2002) 10714.
[36] Y. Sakai, M. Koyanagi, K. Mogi, E. Miyoshi, Surf. Sci. 513 (2002) 272.
[37] G.R. Garda, R.M. Ferullo, N.J. Castellani, Surf. Sci. 598 (2005) 57.
[38] H. Bross, M. Kauzmann, Phys. Rev. B 51 (1995) 17135.
[39] K. Doll, N.M. Harrison, Chem. Phys. Lett. 317 (2000) 282.
[40] Z. Crljen, P. Lazic, D. Sokcevic, R. Brako, Phys. Rev. B 68 (2003) 195411.
[41] J.L.F. Da Silva, K. Schroeder, S. Blugel, Phys. Rev. B 69 (2004) 245411.
[42] A. Bogicevic, K.C. Hass, Surf. Sci. 506 (2002) L237.
[43] Y. Xu, M. Mavrikakis, Surf. Sci. 538 (2003) 219.
[44] N. Perron, N. Pineau, E. Arquis, J.C. Rayez, A. Salin, Surf. Sci. 599 (2005) 160.

[45] S. Stolbov, A. Kara, T.S. Rahman, Phys. Rev. B 66 (2002) 245405.
[46] I. Merrick, J.E. Inglesfield, H. Ishida, Surf. Sci. 551 (2004) 158.
[47] F. Frechard, R.A. van Santen, Surf. Sci. 407 (1998) 200.
[48] A. Martinez, A. Vela, D.R. Salahub, Int. J. Quantum Chem. 63 (1997) 301.
[49] J.E. Fowler, J.M. Ugalde, Phys. Rev. A 58 (1998) 383.
[50] N.E. Schultz, D.G. Truhlar, J. Chem. Theory Comput. 1 (2005) 41.
[51] A. Mananes, F. Duque, F. Mendez, M.J. Lopez, J.A. Alonso, J. Chem. Phys. 119 (2003) 5128.
[52] R.O. Jones, J. Chem. Phys. 99 (1993) 1194.
[53] B.K. Rao, P. Jena, J. Chem. Phys. 111 (1999) 1890.
[54] F. Duque, A. Mananes, Eur. Phys. J. D 9 (1999) 223.
[55] M.D. Deshpande, D.g. Kanhere, I. Vasiliev, R.M. Martin, Phys. Rev. B 68 (2003) 035428.
[56] J. Akola, H. Hakkinen, M. Manninen, Phys. Rev. B 58 (1998) 3601.
[57] J. Akola, M. Manninen, H. Hakkinen, U. Landman, X. Li, L.S. Wang, Phys. Rev. B 62 (2000) 13216.
[58] J. Akola, M. Manninen, Phys. Rev. B 63 (2001) 193410.
[59] V. Kumar, S. Bhattacharjee, Y. Kawazoe, Phys. Rev. B 61 (2000) 8541.
[60] J. VandeVondele, A. De Vita, Phys. Rev. B 60 (1999) 13241.
[61] P. Sen, S. Ciraci, A. Buldum, I.P. Batra, Phys. Rev. B 64 (2001) 195420.
[62] C. Stampfl, J. Neugebauer, M. Scheffler, Surf. Sci. 307–309 (1994) 8.
[63] M. Heinrichsmeier, A. Fleszar, W. Hanke, A.G. Eguiluz, Phys. Rev. B 57 (1998) 14974.
[64] M. Borg, M. Birgersson, M. Smedh, A. Mikkelsen, D.L. Adams, R. Nyholm, C.O. Almbladh, J.N. Andersen, Phys. Rev. B 69 (2004) 235418.
[65] M.J.G. Lee, M. Gensch, A.I. Shkrebtii, Th. Herrmann, W. Richter, N. Esser, Ph. Hofmann, Phys. Rev. B 72 (2005) 14974.
[66] D.R. Jennison, A. Bogicevic, Surf. Sci. 464 (2000) 108.
[67] P.A. Derosa, J.M. Seminario, P.B. Balbuena, J. Phys. Chem. A 105 (2001) 7917.
[68] I. Efremenko, M. Sheintuch, Chem. Phys. Lett. 401 (2005) 232.
[69] F. Illas, N. Lopez, J.M. Ricart, A. Clotet, J.C. Conesa, M. Fernandez-Garcia, J.K. Norskov, J. Phys. Chem. B 102 (1998) 8017.
[70] M. Fernandez-Garcia, J.C. Conesa, A. Clotet, J.M. Ricart, N. Lopez, F. Illas, J. Phys. Chem. B 102 (1998) 141.
[71] Gonzalez, C. Sousa, I. Illas, Surf. Sci. 548 (2004) 209.
[72] V.I. Avdeev, V.I. Kovalchuk, G.M. Zhidomirov, J.L. d'Itri, Surf. Sci. 583 (2005) 46.
[73] S. Stepanyuk, A.N. Baranov, D.I. Bazhanov, W. Hergert, A.A. Katsnelson, Surf. Sci. 482–485 (2001) 1045.
[74] Q.L. Lu, L.Z. Zhu, L. Ma, G.H. Wang, Chem. Phys. Lett. 407 (2005) 176.
[75] N. Andriotis, G. Mpourpakis, G.E. Froudakis, M. Menon, J. Chem. Phys. 120 (2004) 11901.
[76] R. Ferrando, A. Fortunelli, G. Rossi, Phys. Rev. B 72 (2005) 85449.
[77] A.V. Ruban, H.L. Skriver, J.K. Norskov, Phys. Rev. B 59 (1999) 15990.
[78] N. Lopez, J.K. Norskov, Surf. Sci. 477 (2001) 59.
[79] L.A.M.M. Barbosa, D. Loffreda, P. Sautet, Langmuir 18 (2002) 2625.
[80] D.R. Alfonso, A.V. Cugini, D.S. Sholl, Surf. Sci. 546 (2003) 12.
[81] D. Spisak, J. Hafner, Phys. Rev. B 67 (2003) 235403.
[82] O.M. Lovvik, Surf. Sci. 583 (2005) 100.
[83] E. AlShamaileh, C.J. Barnes, A. Wander, J. Phys.: Condens. Matter 15 (2003) 1879.
[84] C. Domain, C.S. Becquart, Phys. Rev. B 65 (2002) 024103.
[85] B.V. Reddy, S.C. Deevi, A.C. Lilly, P. Jena, J. Phys.: Condens. Matter 13 (2001) 8363.
[86] B.V. Reddy, S.N. Khanna, S.C. Deevi, Chem. Phys. Lett. 333 (2001) 465.
[87] B.K. Rao, P. Jena, J. Chem. Phys. 115 (2001) 778.
[88] B.D. Leskiw, A.W. Castleman Jr., C. Ashman, S.N. Khanna, J. Chem. Phys. 114 (2001) 1165.
[89] A. Martinez, L.E. Sansores, R. Salcedo, F.J. Tenorio, J.V. Ortiz, J. Phys. Chem. A 106 (2002) 10630.
[90] B.K. Rao, P. Jena, J. Chem. Phys. 113 (2000) 1508.
[91] S. Chacko, M. Deshpande, D.G. Kanhere, Phys. Rev. B 64 (2001) 155409.
[92] C. Ashman, S.N. Khanna, M.R. Pederson, Phys. Rev. B 66 (2002) 193408.
[93] A. Dhavale, D.G. Kanhere, S.A. Blundell, R.R. Zope, Phys. Rev. B 65 (2002) 85402.
[94] D.E. Bergeron, A.W. Castleman Jr., T. Morisato, S.N. Khanna, Science 304 (2004) 84.
[95] S.N. Khanna, C. Ashman, B.K. Rao, P. Jean, J. Chem. Phys. 114 (2001) 9792.
[96] R.R. Zope, T. Baruah, Phys. Rev. A 64 (2001) 53202.
[97] M. Mayer, G. Pacchioni, N. Rosch, Surf. Sci. 412–413 (1998) 616.
[98] T. Tanaka, T. Nakajima, K. Yamashita, Thin Solid Films 409 (2002) 66.
[99] S. Müller, L.W. Wang, A. Zunger, C. Wolverton, Phys. Rev. B 60 (1999) 16448.
[100] C. Wolverton, X.Y. Yan, R. Vijayaraghavan, V. Ozolins, Acta Mater. 50 (2002) 2187.
[101] M.J. Frisch, G.W. Trucks, H.B. Schlegel, G.E. Scuseria, M.A. Robb, J.R. Cheeseman, V.G. Zakrzewski, J.A. Montgomery Jr., R.E. Stratmann, J.C. Burant, S. Dapprich, J.M. Millam, A.D. Daniels, K.N. Kudin, M.C. Strain, O. Farkas, J. Tomasi, V. Barone, M. Cossi, R. Cammi, B. Mennucci, C. Pomelli, C. Adamo, S. Clifford, J. Ochterski, G.A. Petersson, P.Y. Ayala, Q. Cui, K. Morokuma, D.K. Malick, A.D. Rabuck, K. Raghavachari, J.B. Foresman, J. Cioslowski, J.V. Ortiz, B.B. Stefanov, G. Liu, A. Liashenko, P. Piskorz, I. Komaromi, R. Gomperts, R.L. Martin, D.J. Fox, T. Keith, M.A. Al-Laham, C.Y. Peng, A. Nanayakkara, C. Gonzalez, M. Challacombe, P.M.W. Gill, B. Johnson, W. Chen, M.W. Wong, J.L. Andres, C. Gonzalez, M. Head-Gordon, E.S. Replogle, J.A. Pople, Gaussian 98, Revision A.3, Gaussian, Inc., Pittsburgh, PA, 1998.
[102] A.D. Becke, J. Chem. Phys. 98 (1993) 5648.
[103] J.P. Perdew, K. Burke, Y. Wang, Phys. Rev. B 54 (1996) 16533.
[104] P.J. Hay, W.R. Wadt, J. Chem. Phys. 82 (1985) 270.
[105] W.R. Wadt, P.J. Hay, J. Chem. Phys. 82 (1985) 284.
[106] P.J. Hay, W.R. Wadt, J. Chem. Phys. 82 (1985) 299.
[107] D.R. Lide (Ed.), Handbook of Chemistry and Physics, 76th ed., CRC Press, Boca Raton, FL, 1995.
[108] V. Russier, D.R. Salahub, C. Mijoule, Phys. Rev. B 42 (1990) 5046.
[109] N.M. O/Boyle, J.G. Vos, GaussSum 0.9, Dublin City University, 2005. <http://gausssum.sourceforge.net>.
[110] Spectroscopic tables found at <http://physics.nist.gov/cgi-bin/AtData/main_asd>.
[111] B.N. Cox, C.W. Bauschlicher Jr., Surf. Sci. 115 (1982) 15.